

Vibration-Induced PM and AM Noise in Microwave Components

Archita Hati, Craig W. Nelson, and David A. Howe, *Senior Member, IEEE*

Abstract—The performance of microwave components is sensitive to vibrations to some extent. Aside from the resonator, microwave cables, and connectors, bandpass filters, mechanical phase shifters, and some nonlinear components are the most sensitive. The local oscillator is one of the prime performance-limiting components in microwave systems ranging from simple RF receivers to advanced radars. The increasing present and future demand for low acceleration sensitive oscillators, approaching $10^{-13}/g$, requires a reexamination of sensitivities of basic nonoscillatory building-block components under vibration. The purpose of this paper is to study the phase-modulation (PM) noise performance of an assortment of oscillatory and nonoscillatory microwave components under vibration at 10 GHz. We point out some challenges and provide suggestions for the accurate measurement of vibration sensitivity of these components. We also study the effect of vibration on the amplitude-modulation (AM) noise.

I. INTRODUCTION

HIGH-PRECISION oscillators have significant applications in modern communication and navigation systems, radars, and sensors mounted in unmanned aerial vehicles, helicopters, missiles, and other dynamic platforms. These systems are gaining use in the tens of gigahertz microwave spectrum and must meet their performance requirements even when subjected to severe dynamic environmental conditions. In most applications, the acceleration experienced by a microwave oscillator is in the form of vibration, which can introduce mechanical deformations that deteriorate the oscillator's otherwise low phase-modulation (PM) noise [1]–[3]. This degrades the performance of the entire electronic system that depends on this oscillator's low phase noise.

The acceleration sensitivity of an oscillator originates most commonly from deformations induced by acceleration in the frequency-determining element, the resonator. The resonant frequency of a resonator depends on its dimensions, thus mapping any changes in size to frequency. The frequency shift due to physical deformation of resonator is a linear effect. There are also frequency shifts due to nonlinear effects that arise from the nonlinear elasticity in the deformed resonator material [4]. This behavior may become pronounced when vibration levels exceed one or more thresholds. The effect of such nonlinearity is that a

single-frequency vibration spectrum causes not only a corresponding single-frequency spur in the phase noise spectrum of the device, but also produces harmonically related frequency spurs [2]. Symmetry, either in the resonator geometry or in the mounting configuration can lead to lower acceleration sensitivity [4]–[10]. The acceleration sensitivity can further be reduced by passive isolation as well as active cancellation of vibration-induced noise [11]–[15].

Vibration also causes mechanical deformations in non-frequency-determining electronic components that then cause phase fluctuations [2], [16], [17]. In general, these effects are more prominent in higher-frequency oscillators, due to increased signal phase sensitivity to mechanical deformation and decreased resonator quality factor [2]. If these phase fluctuations are inside the oscillator feedback loop, they convert to frequency fluctuations via Leeson's effect [18] within the resonator half-bandwidth (HBW). In recent years, resonator and oscillator frequency sensitivity to vibration has improved to a point where the phase sensitivity of nonoscillatory components cannot be overlooked [11]–[15]. Coaxial cables and connectors, bandpass filters, mechanical phase shifters, and amplifiers are the most sensitive, particularly at microwave frequencies [17], [19]. The increasing present and future demand for low vibration-sensitive oscillators, approaching $10^{-13}/g$ ($1 g$ is the acceleration of gravity near the earth's surface, approximately 9.8 m/s^2), requires a reexamination of sensitivities of basic nonoscillatory building block components under vibration.

The purpose of this paper is to study the performance of an assortment of oscillatory and nonoscillatory components under vibration normalized to a microwave frequency of 10 GHz. A large number of studies have been done for quartz oscillators at megahertz frequencies, with references in [12], and therefore are not taken into consideration for the vibration test in this paper. We first introduce the relationship between acceleration sensitivity and phase noise in Section II. In Section III, we discuss the PM and AM noise measurement techniques, point out some challenges, and provide a few suggestions for accurate measurement in the presence of vibration. We also present AM and PM noise performance of some nonoscillatory components. In Section IV, we present the acceleration sensitivity results for different classes of oscillators, and finally a summary is given in Section V.

II. ACCELERATION SENSITIVITY AND PHASE NOISE

An oscillator's sensitivity to vibration is traditionally characterized by acceleration sensitivity, which is the

Manuscript received February 5, 2009; accepted June 26, 2009. Work of U.S. government, not subject to copyright. Commercial products are identified in this document only for complete technical description; no endorsement is thereby implied.

The authors are with the National Institute of Standards and Technology, Time and Frequency Division, Boulder, CO (e-mail: archita@boulder.nist.gov).

Digital Object Identifier 10.1109/TUFFC.2009.1288

normalized frequency change per unit g . When an oscillator is subjected to acceleration, its resonant frequency shifts. The frequency shift, $\Delta f(t)$, which is proportional to the magnitude of the time-dependent acceleration and depends on the direction of acceleration, is given by a fractional-frequency change $y(t)$ as [1]

$$y(t) = \frac{\Delta f(t)}{f_0} = \vec{\Gamma} \cdot \vec{a}(t) = \sum_i \Gamma_i a_i(t), \quad (1)$$

where f_0 is the frequency of the oscillator with no acceleration, $\vec{\Gamma}$ is the acceleration sensitivity vector, and $\vec{a}(t)$ is the applied acceleration vector. Γ_i and a_i are the components of these 2 vectors in the i ($i = x, y, \text{ or } z$) direction. When the direction of applied acceleration is parallel to the axis of the acceleration sensitivity vector, it will have the greatest effect on frequency shift. The associated power spectral density (PSD) of (1) is

$$S_y(f) = \sum_i \Gamma_i^2 S_{a_i}(f), \quad 1/\text{Hz}, \quad (2)$$

where $S_y(f)$ and $S_a(f)$ are the PSD of rms fractional frequency fluctuations and rms acceleration, respectively. $S_a(f)$ should not be confused with $S_\alpha(f)$, which is the PSD of amplitude fluctuations. For simplicity, we will now drop the subscript i and consider contributions only along a single axis. For a low modulation index, the single sideband phase noise, $L(f_v)$ at any vibration frequency f_v is related to acceleration sensitivity as

$$L(f_v) \equiv \frac{1}{2} S_\phi(f_v) = \frac{1}{2} S_y(f_v) \left(\frac{f_0}{f_v} \right)^2 = \frac{1}{2} S_a(f_v) \left(\frac{\Gamma f_0}{f_v} \right)^2 \quad (3)$$

or, in decibels (dB),

$$L(f_v) = 20 \log \left[\Gamma \frac{f_0}{f_v} \sqrt{\frac{S_a(f_v)}{2}} \right], \quad \text{dBc/Hz}. \quad (4)$$

Eq. (4) can be rearranged to obtain

$$\Gamma = \frac{f_v}{f_0} \sqrt{\frac{2}{S_a(f_v)}} 10^{L(f_v)/20} \quad 1/g. \quad (5)$$

Under random vibration, the acceleration is randomly distributed over a range of frequencies and represented by its power spectral density, $S_a(f_v)$ in units of g^2 per hertz (g^2/Hz). Also, for random vibration, $L(f_v)$ is expressed in units of decibels relative to the carrier power per unit bandwidth (dBc/Hz) and Γ is calculated from (5). On the other hand, when the vibration is sinusoidal vibration, Γ is determined from

$$\Gamma = \frac{2f_v}{a_{\text{peak}} f_0} 10^{L(f_v)/20}, \quad (6)$$

where a_{peak} is the peak sinusoidal acceleration in units of g and $L(f_v)$ is the phase noise power spectrum of the sinu-

soidal modulation expressed in units of decibels relative to the carrier power (dBc, not dBc/Hz).

The sum of acceleration sensitivity squared in all 3 axes gives the total acceleration sensitivity, or gamma (Γ_{tot}), and is given by [2], [20]

$$\Gamma_{\text{tot}} = \sqrt{\Gamma_x^2 + \Gamma_y^2 + \Gamma_z^2}. \quad (7)$$

Γ_{tot} of an oscillator can be calculated from (7) once the PM noise of the oscillator is measured for all 3 axes.

Now, when a nonoscillatory component is subject to acceleration, it causes a change in phase of the signal traveling through it, which is given by

$$\psi(t) = \vec{\Gamma}_\psi \cdot \vec{a}, \quad (8)$$

where $\vec{\Gamma}_\psi$ is the acceleration sensitivity vector of phase and expressed in units of radians per g . Following the same mathematical steps as described in (2) to (4), we can write the acceleration sensitivity due to phase fluctuations as

$$\begin{aligned} \Gamma_\psi(f_v) &= \sqrt{\frac{2}{S_a(f_v)}} 10^{(L(f_v)/20)} \\ &= \frac{1}{\sqrt{S_a(f_v)}} 10^{(S_\psi(f_v)/20)} \quad \text{rad/g}. \end{aligned} \quad (9)$$

When these nonoscillatory components (resonator, amplifier, filter, cables, or phase shifter) are placed inside the oscillator loop, the vibration induced double sideband phase noise of the oscillator can be written as [18], [21]

$$S_\phi(f_v) = \left[1 + \left(\frac{f_0}{2Q_{\text{eff}} f_v} \right)^2 \right] S_{\psi\text{-loop}}(f_v) + S_{\psi\text{-PC}}(f_v). \quad (10)$$

$S_{\psi\text{-loop}}(f_v)$ and $S_{\psi\text{-PC}}(f_v)$ are, respectively, the combined phase noise of loop components and the post-loop components under vibration. Q_{eff} is the effective quality factor (Q) of the entire feedback loop, which is equal to half of the slope of the transmission phase response ($d\varphi/dy$) at resonance [21]. Effective Q is used for all resonant components in this paper. A resonator in an open loop condition maps frequency fluctuations of its resonance to phase fluctuations on a signal passing through it, and when an oscillator is built with this resonator, these phase fluctuations convert back to frequency fluctuations of the oscillator output signal. In other words, the frequency fluctuations of the resonator convert directly to the frequency fluctuations of the oscillator. So, if the resonator is the only contributor to loop Q , (10) can be rewritten as

$$\begin{aligned} S_\phi(f_v) &= \left(\frac{f_0}{f_v} \right)^2 S_{y\text{-res}}(f_v) + \left[1 + \left(\frac{f_0}{2Q_{\text{res}} f_v} \right)^2 \right] S_{\psi\text{-loop}}(f_v) \\ &\quad + S_{\psi\text{-PC}}(f_v), \end{aligned} \quad (11)$$

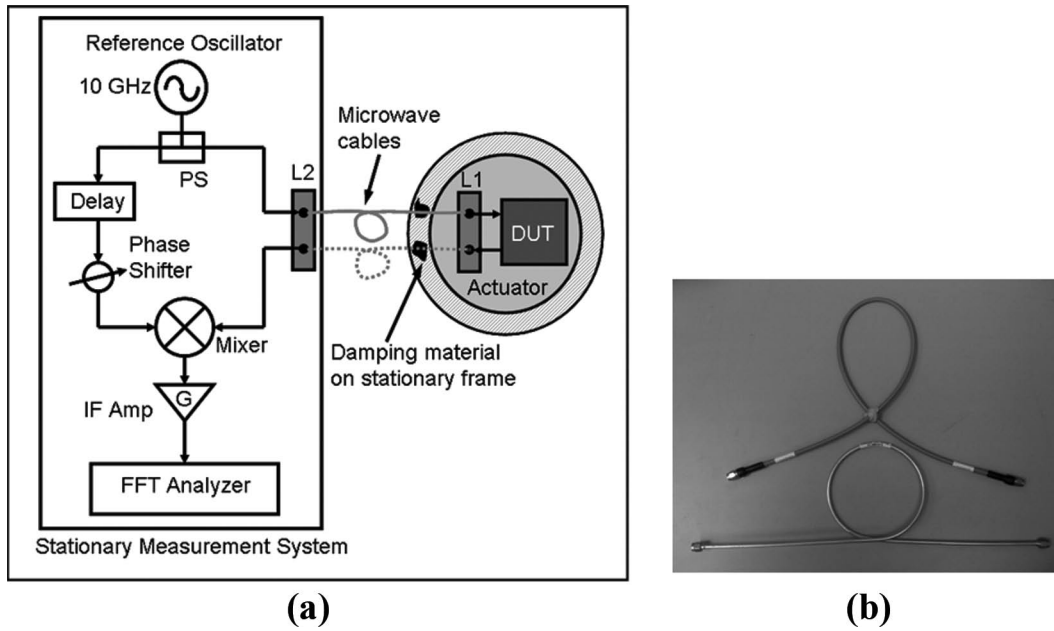


Fig. 1. (a) Block diagram of an experimental setup for residual phase-modulation noise measurement of components under vibration. PS = power splitter, DUT = device under test, IF Amp = intermediate frequency amplifier, L1 and L2 = L-shaped brackets. (b) Typical cables used for vibration test.

where $S_{y\text{-res}}(f_v)$ and Q_{res} are PSD of rms fractional frequency fluctuations and effective Q of the resonator, respectively. Using (3), (6), (9), and (11), a relationship between acceleration sensitivity of an oscillator (Γ_{osc}) in terms of acceleration sensitivity of resonator (Γ_{res}), loop components ($\Gamma_{\psi\text{-loop}}$) and post-loop components ($\Gamma_{\psi\text{-PC}}$) can be written as

$$\Gamma_{\text{osc}}^2 = \Gamma_{\text{res}}^2 + \left[\left(\frac{f_v}{f_0} \right)^2 + \frac{1}{4Q_{\text{res}}^2} \right] \Gamma_{\psi\text{-loop}}^2(f_v) + \left(\frac{f_v}{f_0} \right)^2 \Gamma_{\psi\text{-PC}}^2(f_v). \quad (12)$$

This expression shows that the effect of acceleration sensitivity (Γ_{ψ}) of various nonoscillatory loop components on the acceleration sensitivity of an oscillator is reduced by $2Q_{\text{res}}$ inside the resonator HBW.

III. EFFECT OF VIBRATION ON NONOSCILLATORY DEVICES AT 10 GHz

A. PM Noise

Fig. 1(a) is a block diagram of a PM noise measurement system used to measure the residual noise of a nonoscillatory device such as a bandpass filter or amplifier as well as a cable and connector under vibration. The output power of a reference oscillator is split into 2 paths. One path is used to drive the device under test (DUT) mounted to an actuator, and the other path is connected to a delay line. The delay is chosen so that the delay introduced in one path is equal to the delay in the other path. A phase

shifter is used to set phase quadrature, or 90 degrees, between 2 paths, and the resulting signals are connected to a double-balanced mixer acting as a phase detector. The baseband signal at the output of the phase detector is amplified and measured on a fast Fourier transform (FFT) analyzer. Because the delays in the 2 signal paths are equal, the PM noise from the reference oscillator is equal and correlated in each path and thus cancels [22]. At the output of the mixer, the phase fluctuations from the vibrating DUT and its connecting cables are detected because they appear differentially at the 2 inputs of the mixer. A low-noise phase detector and IF amplifier are chosen for this measurement, and their noise contributions are much lower than the dominating vibration-induced noise of the DUT and cables.

1) *Cable Considerations:* To measure the acceleration sensitivity of a DUT accurately, it is important to know the noise floor of the measurement system. The main contributors to the vibration-induced PM noise floor are the coaxial cables, as illustrated by the gray curves in Fig. 1(a), connected between the stationary measurement system and the actuator. Under vibration, these cables flex, causing localized distortions in the coaxial structure that lead to modulations of the propagation parameters of the cable. Piezoelectric effects in coaxial cables can also be involved [23]. The main challenge is to obtain a reproducible low noise floor set by these flexing cables at close-to-carrier offset frequencies. For the noise floor measurement, the DUT is replaced by an 8-cm-long semirigid coaxial cable whose solid outer conductor diameter is 0.358 cm. The measured noise floor is dependent on the configuration and tension of the cables running between the vibrating and stationary reference frames; changes in the

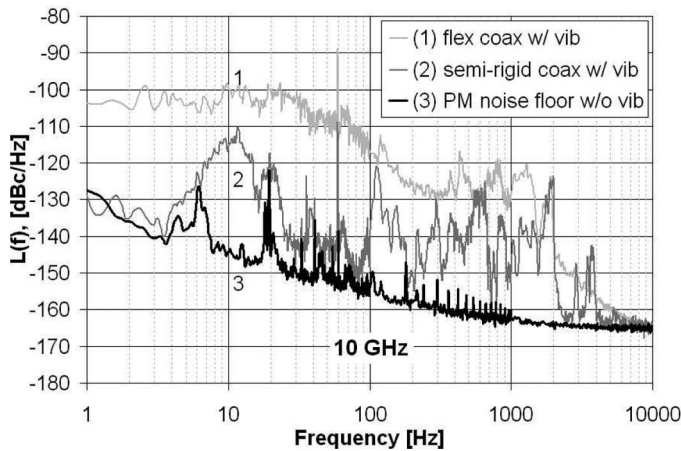


Fig. 2. Residual phase-modulation (PM) noise floor of the measurement system under vibration for semirigid coaxial and braided-shield, flexible coaxial. The device under test is replaced by 8-cm-long semirigid coaxial cable for this test. A random vibration with $S_a(f_v) = 1.0 \text{ mg}^2/\text{Hz}$ is used for $10 \text{ Hz} \leq f_v \leq 2000 \text{ Hz}$. The bottom curve shows the noise floor measured under no vibration. Narrow spurs are power-line EMI pick-up and should be ignored.

configuration can cause the noise to vary by anywhere from 10 dB to 30 dB. The configuration used for these measurements is shown in Fig. 1(a). It uses 2 L-shaped brackets (L1 and L2) each containing 2 SMA bulkhead connectors, one located on the stationary measurement system and other on the actuator. The microwave cables run between stationary and vibrating reference frames via these SMA connectors. Different amounts of cable slack, tension, and damping are used to obtain the best noise floor. It is also worthwhile to mention that use of clay-like adhesive poster putty as a damping material is found to be very effective in reducing the vibration-induced noise in the cables. The advantage of this configuration is that, once the lowest noise floor is achieved, the DUT can easily be replaced without affecting the system noise floor.

Also, we find that the noise floor can vary significantly from one type and brand of cables to another. To test this, we measured the noise floor using several different types of cables available in the laboratory and noticed significant differences in the results. In Fig. 2, the residual PM noise results at 10 GHz of 2 cable types are shown. First, the noise floor is measured with semirigid coaxial cables whose outer solid conductor diameter is 0.358 cm, each 46 cm long, represented by solid and dotted gray curves in Fig. 1(a). Then, one of the semirigid coaxial cables represented by the dotted gray curve is replaced with a braided-shield flexible coaxial cable of the same length, and the noise floor is measured again. Fig. 1(b) shows the picture of 2 cable types used for vibration tests. A random vibration profile of acceleration PSD of $1.0 \text{ mg}^2/\text{Hz}$ (rms) is used between $10 \text{ Hz} \leq f_v \leq 2000 \text{ Hz}$. This range of vibration frequencies is the range for our vibration table, adequately covering smaller ranges associated with most applications.

The results show that the noise floor can vary by 10 dB to 30 dB, depending on the cable types; therefore, extra

care must be taken in selecting the cables for vibration-induced noise measurements. Among the samples of coaxial cables tested, we find that the vibration sensitivity is lowest for the semirigid coaxial cable whose solid outer conductor diameter is 0.358 cm. However, this sensitivity to vibration is not low enough to measure an oscillator whose acceleration sensitivity is $1 \times 10^{-13}/\text{g}$. For perspective, an oscillator at 10 GHz under random vibration of $1.0 \text{ mg}^2/\text{Hz}$ (rms) will produce single sideband phase noise of -113 and -153 dBc/Hz, respectively, at 10 and 1000 Hz offset frequencies, which is below the noise floor of the semirigid cable under vibration. Fig. 2 also indicates that the PM noise of the vibrating cable is not flat with offset frequency. This may be due to a low-pass filtering effect of the damping material as well as the loop structure, shown in Fig. 2(b), bent into the cable on the overall mechanical frequency response.

2) *DUT Considerations*: Measuring the acceleration sensitivity of a DUT is challenging. For accurate measurements the following precautions should be taken:

- Experiment with different types of connecting cables as well as different amounts of cable slack or tension between the stationary and vibrating reference frames to obtain the best noise floor.
- Rigidly mount the DUT on the vibration table to avoid any mechanical resonance inside the frequency range of interest.
- Properly secure the cables to minimize flexing and strain due to vibration. It is also important to secure the power leads for the DUT properly.
- Reduce the acoustic noise and external vibration in the test area.
- The vibration actuator often has cooling fans; prevent this airflow from disturbing the connecting cables, DUT, or measurement-system components.
- No other components except the DUT and accelerometer should be mounted on the shaker.
- If possible, use 1- to 3-dB attenuators at the connector interfaces to minimize the effect of voltage-standing-wave-ratio (VSWR)-induced mechanical and multipath phase fluctuations.
- Ground loops interact with magnetic and electric fields generated by the vibrating actuator. Minimizing the ground loops is of utmost importance for accurate measurements.
- Check the noise floor between the measurements by replacing the DUT with a short cable.

After establishing a low noise floor, 2, 10-GHz band-pass cavity filters of different Q as shown in Fig. 3(a) are tested under random vibration along the z axis. The effective Qs of these 2 filters are approximately 3739 and 320. A random vibration profile of acceleration PSD $1.0 \text{ mg}^2/\text{Hz}$ (rms) for offset-frequency range 10 Hz to 2000 Hz is used. Fig. 4 shows the PM noise floor of the measurement system as well as the PM noise of the filters under vibra-

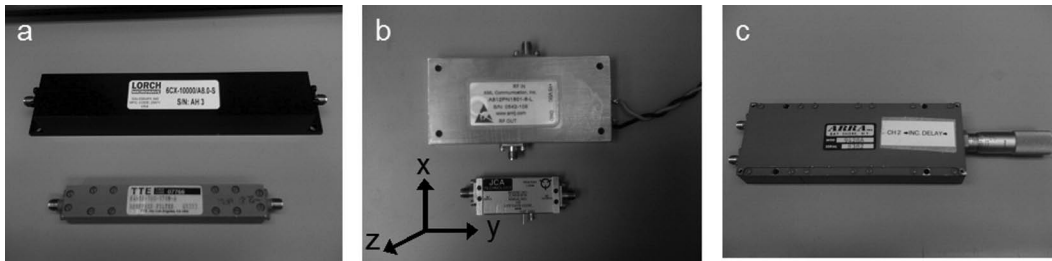


Fig. 3. Picture of the nonoscillatory components used for vibration tests at 10 GHz. (a) High-Q (3739) and low-Q (320) bandpass filters, (b) amplifiers, (c) phase shifter. Arbitrary x and y axes are chosen in the plane of the page, and the z axis is normal to the device top surface.

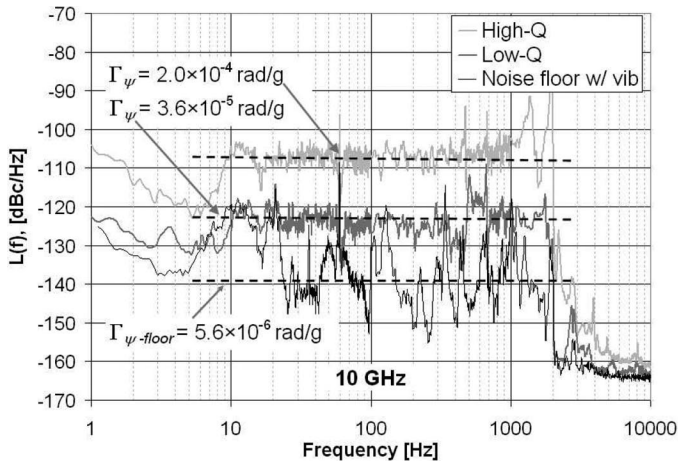


Fig. 4. Phase-modulation (PM) noise of 2, 10-GHz bandpass cavity filters under vibration along the z axis. A random vibration with $S_a(f_v) = 1.0 \text{ mg}^2/\text{Hz}$ is used for $10 \text{ Hz} \leq f_v \leq 2000 \text{ Hz}$. The bottom curve shows the PM noise floor set by flexing of cables under vibration. The z -axis acceleration sensitivities (Γ_ψ) of high and low Q filters are, respectively, $2.0 \times 10^{-4} \text{ rad/g}$ [for $L(f) = -107 \text{ dBc/Hz}$] and $3.6 \times 10^{-5} \text{ rad/g}$ [for $L(f) = -122 \text{ dBc/Hz}$].

tion. The sensitivity of these filters to vibration is found to be very dependent on the amount of stress applied on them by the mounting fixture while securing them on the vibration table. The results presented in Fig. 4 are the lowest obtained under certain conditions. The z -axis acceleration sensitivity of these filters calculated from (9) is also indicated in Fig. 4.

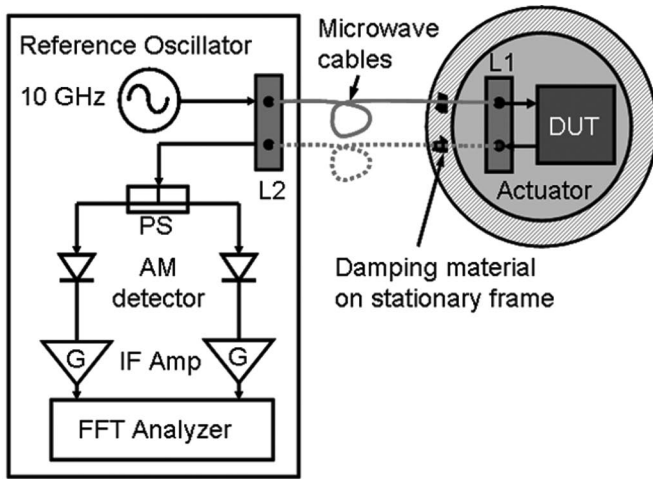
The result shows that the filter with higher Q is more sensitive to vibration. One possible reason is due to the fact that the transfer function phase of a high-Q filter has a steeper slope at its center frequency. Any vibration that modulates the resonant structure of the filter also modulates the center frequency and thus the phase shift through the filter. The phase slope is proportional to the filter Q; this causes the high-Q filter to be more sensitive to small mechanical distortions under vibration. However, the acceleration sensitivity does not necessarily depend solely on the Q of a filter. A cavity filter is a multipole or higher-order filter consisting of several resonators. These resonators are distributed in the filter network, each of which modulates the signal. The Q can be increased by increasing the number of resonators, which may make it more vibration sensitive. In other words, increasing the

number of stages of a filter increases the sensitivity to mechanical stress. Fig. 4 indicates the fact that Q is not the only dominant factor in the filters' vibration sensitivities. Because the phase noise difference between the 2 filters is $\sim 17 \text{ dB}$, which is less than $20\log(3739/320) = 21.4 \text{ dB}$, this means that structural effects such as the shape and size of the cavity housing and other mechanical processes are playing a role, making the high-Q filter better than expected, the low-Q filter worse than expected, or a combination of both.

Finally, the PM noises of a few amplifiers and a mechanical phase shifter at 10 GHz are also measured under vibration. For these components, the PM noise is either lower than or equal to the noise floor of the connecting cables under vibration. As a result, an accurate measurement is not possible. However, it can be concluded from the experimental results that the acceleration sensitivity (Γ_ψ) of the phase shifter and amplifiers under test is no greater than $5.6 \times 10^{-6} \text{ rad/g}$, as shown in Fig. 4.

B. AM Noise

The flexing of coaxial cables due to vibration changes the structure of the cable, which not only modulates the phase of the transmitting signal but also modulates its amplitude [17]. However, unlike vibration-induced PM noise, the AM noise can be less of a problem because this effect can be reduced by amplitude compressing or clipping the signal. Fig. 5 shows a block diagram of the cross-correlated measurement system used to measure AM noise [22] of cables, amplifiers, and filters under vibration. The output of the reference oscillator is fed to the DUT mounted on the actuator. The signal returning from the DUT is split into 2 paths, each containing the vibration-induced AM noise of the DUT and cables plus the AM noise of the stationary reference oscillator. These signals are fed to a 2-channel, cross-correlation FFT analyzer. The advantage of this technique is that only the AM noise coherent to both channels, i.e., the noise of the oscillator, vibrating cables, and DUT, averages to a finite value. The time average of the incoherent noise processes, such as the AM detectors and IF amplifiers, approaches zero as the number of averages used in cross-spectrum increases. An oscillator of very low AM noise is used for this test so as not to dominate the DUT noise.



Stationary Measurement System

Fig. 5. Block diagram of an experimental setup for amplitude-modulation (AM) noise measurement of components under vibration. PS = power splitter; DUT = device under test; IF Amp = intermediate frequency amplifier.

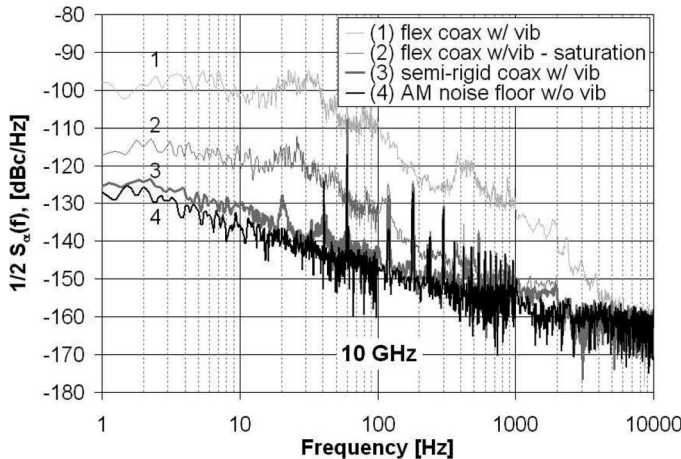


Fig. 6. Amplitude-modulation (AM) noise floors of the measurement system for semirigid and braided shield flexible coaxial cable under vibration at 10 GHz. A random vibration with $S_a(f_v) = 1.0 \text{ mg}^2/\text{Hz}$ is used for $20 \text{ Hz} \leq f_v \leq 2000 \text{ Hz}$. The second curve from the top shows the reduction in vibration-induced AM noise after the signal is saturated by a stationary amplifier. $S_\alpha(f)$ is the double sideband AM noise.

First, the DUT is replaced with an 8-cm-long semirigid coaxial cable, and the vibration-induced AM is measured for the same 46-cm-long semirigid and braided-shield flexible cables as those used for PM noise measurement. The vibration-induced AM noise is found to be negligible for semirigid cables; however, it is significant for braided-shield flexible cable. The AM vibration noise of flexible cable can be reduced by following it with a saturated amplifier. A stationary low-AM-noise amplifier in saturation is used before the power splitter, and a reduction of almost 20 dB is observed, as shown in Fig. 6. These results indicate that, when selecting cables either for a vibration measurement or for low vibration-sensitive design, it is equally important to measure both vibration-induced AM and PM noise. Further nonlinear processing of the signal,

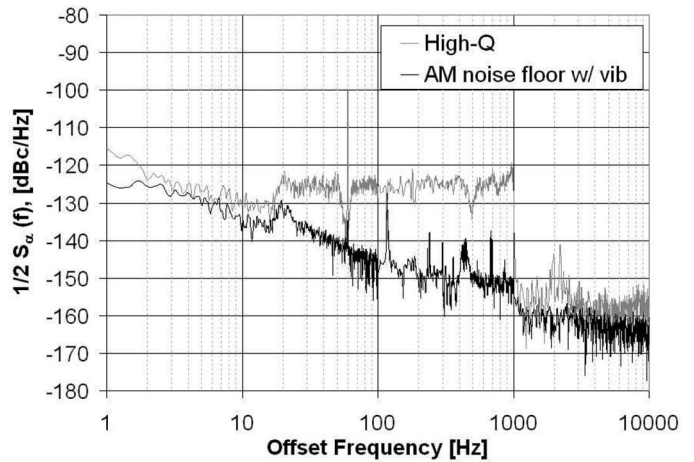


Fig. 7. Amplitude-modulation (AM) noise performance of a bandpass cavity filter at 10 GHz under vibration. The effective Q of the filter is approximately 3739. A random vibration with $S_a(f_v) = 1.0 \text{ mg}^2/\text{Hz}$ is used for $20 \text{ Hz} \leq f_v \leq 2000 \text{ Hz}$.

such as mixing, may cause inadvertent AM-to-PM conversion of vibration-induced AM noise.

Next, the short semirigid coaxial is replaced by a DUT, in this case, bandpass cavity filters; see Fig. 3(a). The AM noise contribution of the low-Q (320) filter is below the AM noise floor. Fig. 7 shows only the AM noise added by the high-Q (3739) filter under vibration. If this filter is used inside an oscillator loop, the effect of AM noise will be reduced significantly due to saturation of the signal by the loop amplifier. However, in a system where the bandpass filter is used as a post filter, often known as spectrum cleanup filter, under vibration such filters can amplitude-modulate the signals passing through them and add significant AM noise to a frequency source of low AM noise. Hence, these spectrum cleanup filters must be selected carefully in systems subject to vibration.

IV. ACCELERATION SENSITIVITY OF DIFFERENT CLASSES OF OSCILLATORS

Fig. 8 shows the setup used to measure acceleration sensitivity of different microwave oscillators. A direct digital PM noise measurement system [24] is used that utilizes fast analog-to-digital converters to digitize the input RF signal and perform down-conversion and phase detection functions by digital signal processing. The oscillator under test is mounted on the actuator, with the output going to one input of a mixer. This output is then mixed with a stationary very-low-PM-noise oscillator to generate a beat frequency between 1 MHz to 30 MHz for digitizing directly. A low-noise 10-MHz quartz crystal oscillator serves nicely as the digitizer's reference.

First, we investigate how the acceleration sensitivity of nonoscillatory components translates to the acceleration sensitivity of an oscillator when these components are placed inside the oscillator loop. We build 2 simple oscillators at 10 GHz as shown in Fig. 9, one using a high-Q

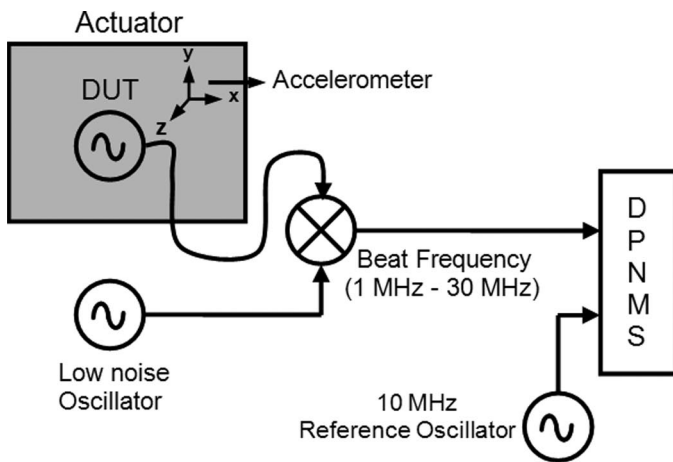


Fig. 8. Block diagram of an experimental setup for measuring acceleration sensitivity of an oscillator. DPNMS = direct-digital phase noise measurement system; DUT = device under test.

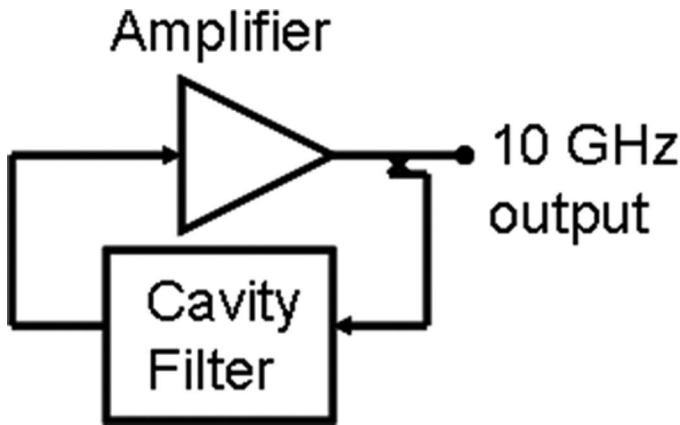


Fig. 9. Block diagram of a simple loop oscillator at 10 GHz. The band-pass cavity filter acting as a resonator is the most vibration-sensitive element in the loop.

(3739) cavity filter and another using a low-Q (320) cavity filter as the resonators. All other loop components are kept identical for both oscillators. The PM noise of the 2 oscillators are measured with and without vibration along the z axis, and the results are shown in Fig. 10. It shows that when the oscillators are at rest, the difference in their PM noise is approximately 20 dB, which is in close agreement with the result predicted from Leeson's model. The vibration sensitivity of these oscillators calculated from (5) using $L(f_v)$ of Fig. 10, indicates that the high-Q oscillator is slightly less sensitive to vibration.

We also calculate Γ_{osc} theoretically from (12) by equating Γ_{osc} to Γ_{res} , ignoring the small contributions of all other loop components. Because the applied vibration is within the resonator HBW, Γ_{res} is obtained by dividing Γ_{ψ} of the cavity filter by $2Q_{\text{res}}$. The theoretical result agrees with the experimental finding that the high-Q oscillator is less sensitive to vibration. However, for both oscillators, there are slight differences in the experimental and theoretical value of Γ_{osc} . This difference, which is less than a factor of 2, can be well explained as follows. As mentioned earlier,

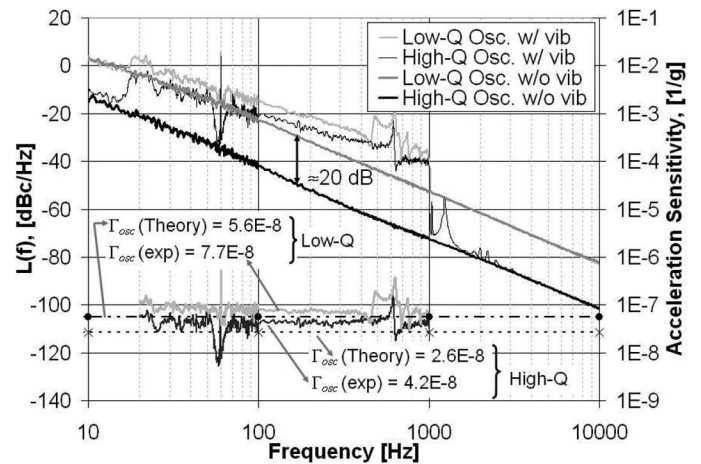


Fig. 10. The phase-modulation (PM) noise of 2 oscillators with and without vibration along the z axis. The secondary y axis represents the acceleration sensitivity of the oscillator. A random vibration with $S_a(f_v) = 1.0 \text{ mg}^2/\text{Hz}$ is used for $20 \text{ Hz} \leq f_v \leq 2000 \text{ Hz}$. $\Gamma_{\psi} = 2.0 \times 10^{-4} \text{ rad/g}$ for high-Q filter and $\Gamma_{\psi} = 3.6 \times 10^{-5} \text{ rad/g}$ for low-Q filter is used for Γ_{osc} (theory) calculation.

the vibration sensitivity of these filters are very sensitive to the stress applied on them by the mounting fixture. It is quite possible that the amount of stress applied on the filters when they are mounted inside the oscillator loop is different from the stress used for the residual noise measurement, resulting in vibration sensitivity of high-Q and low-Q filters higher than that used for the calculation.

Next, we measured the vibration sensitivity of commercial and custom oscillators. Fig. 11 shows different types of oscillators chosen for the vibration test, namely, low- and high-PM noise dielectric resonator oscillators (DROs) at 10 GHz, a silicon germanium (SiGe) amplifier-based surface transverse wave (STW) oscillator at 2.5 GHz [25], and a TE_{023} mode air-dielectric ceramic-cavity resonator oscillator (ACCRO) at 10 GHz [26]. An STW oscillator is chosen because this is a very low noise oscillator with a stiff resonator in the frequency range 1 to 3 GHz. Below 1 GHz, SAW oscillators perform well [27], and above 3 GHz, DROs provide the best compromise between performance and cost. There are several other commercially available oscillators above 3 GHz that have extremely low phase noise, but they are large, specialized, and expensive by comparison.

At first, the PM noise of DRO-1, STW, and ACCRO is measured without vibration, and then they are subjected to random vibration along the z axis. Figs. 12 and 13 show the PM noise and z -axis acceleration sensitivity of these oscillators, respectively; the acceleration sensitivity of the STW oscillator is 2 orders of magnitude lower than that of the DRO.

Further, the acceleration sensitivities of 2 DROs of comparable size and weight but different PM noise are compared. These DROs at 10 GHz are subjected to a random vibration along 3 axes independently. For DRO-1, the effect of random vibration in the x and y axes is not noticeable, because the PM noise of the stationary DRO

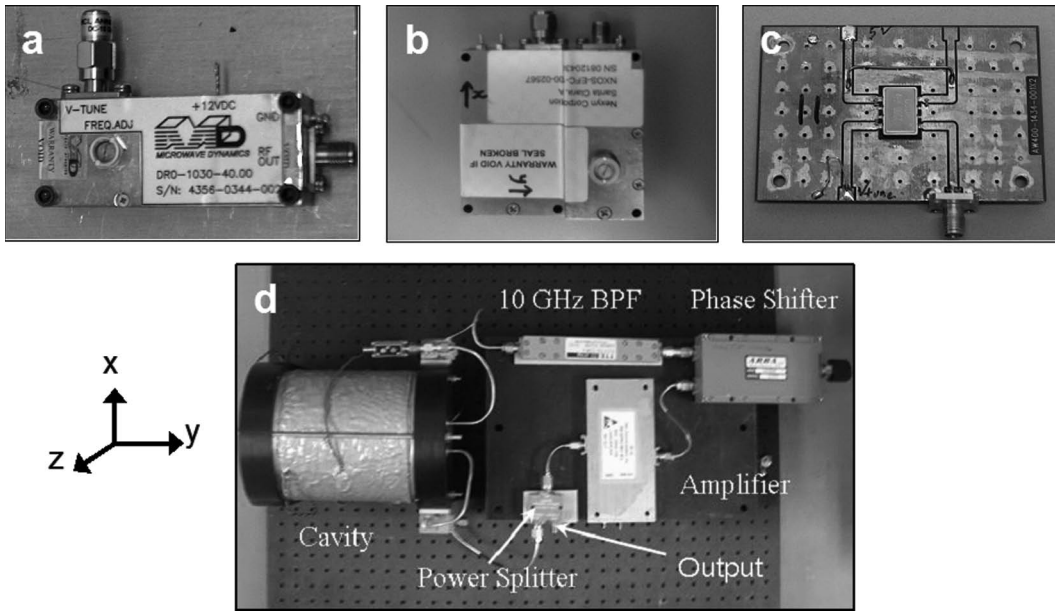


Fig. 11. Pictures of 4 different types of oscillators used for vibration tests: (a) dielectric resonator oscillator (DRO-1) with high phase-modulation noise, (b) DRO-2 with low PM noise, (c) surface transverse wave (STW) oscillator, (d) air-dielectric ceramic-cavity resonator oscillator (ACCRO). Arbitrary x and y axes are chosen in the plane of the page, and the z axis is normal to the device top surface.

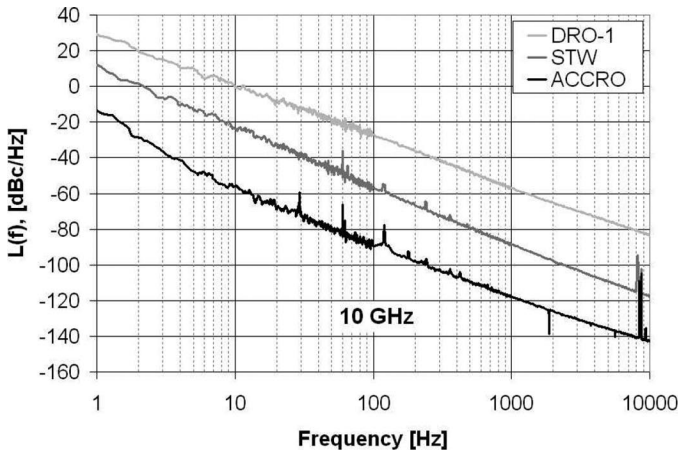


Fig. 12. Phase-modulation (PM) noise of 3 different oscillators at 10 GHz without vibration. For direct comparison, the PM noise of a 2.5-GHz STW oscillator is normalized to 10 GHz.

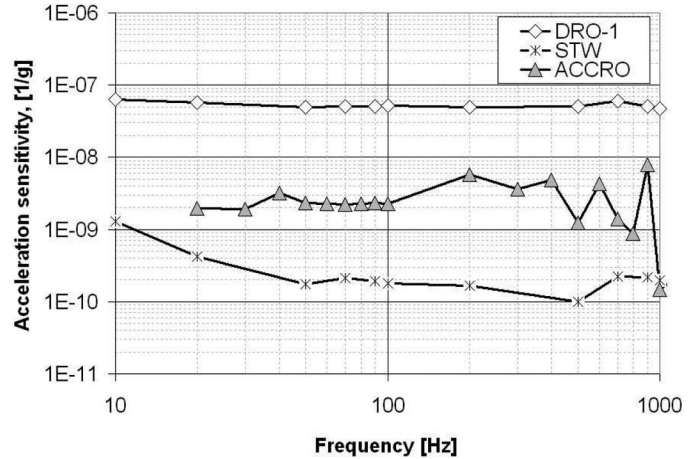


Fig. 13. Comparison of z -axis acceleration sensitivity of different oscillators. A peak acceleration (a_{peak}) of 1 g is used.

is significantly higher than the noise induced by random vibration. To measure the acceleration sensitivity in all 3 axes, the DRO is subjected to sinusoidal vibration with higher g -levels at different spot frequencies. Figs. 14 and 15, respectively, show the PM noise and acceleration sensitivity of these DROs. These results show that a low-noise oscillator at rest is not necessarily the best choice for certain applications on a vibrating platform.

V. DISCUSSION

Structure-borne vibration is routine for many applications, causing an increase in PM noise of oscillators that disables or degrades the performance of many systems. Therefore, it is very important to select components that

show low-phase changes under vibration to build a system with low-vibration sensitivity.

In this paper, the acceleration sensitivity of several microwave components is reported. We find that the coaxial cables that run between the vibrating platform and the stationary measurement system set the PM and AM noise floor. Depending on the cable type, the noise floor can vary anywhere from 10 dB to 30 dB; therefore, extra care must be taken in selecting coaxial cables. We also find that acceleration sensitivity of some components is dependent on mechanical stress; symmetry in the mounting configuration can lead to lower acceleration sensitivity. Our finding also shows that a low-noise oscillator at rest is not necessarily the best choice for certain applications on a vibrating platform. Vibration also affects the AM noise of nonoscillatory components, and sometimes vibration-

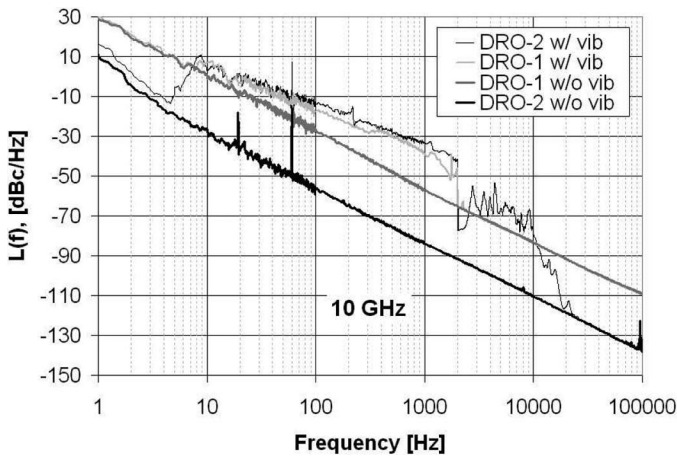


Fig. 14. Phase-modulation (PM) noise of DRO-1 and DRO-2 with and without vibration along the z axis. A random vibration with $S_d(f_v) = 1.0 \text{ mg}^2/\text{Hz}$ is used for $10 \text{ Hz} \leq f_v \leq 2000 \text{ Hz}$.

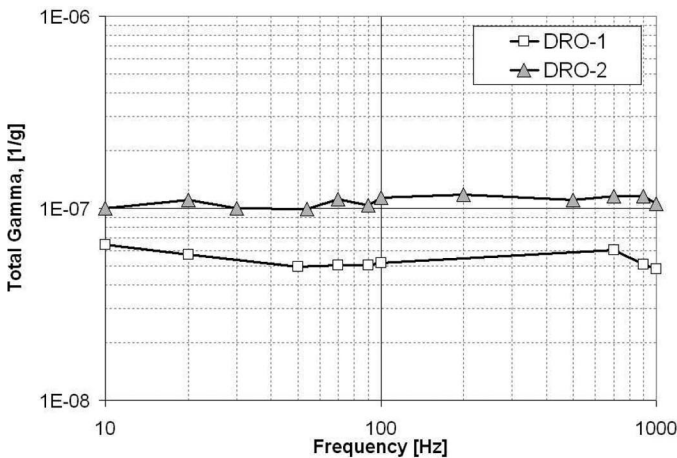


Fig. 15. Plot of total gamma (Γ_{tot}) for the DROs. The lower phase-modulation (PM) noise oscillator has higher acceleration sensitivity.

induced AM noise can be greater than vibration-induced PM noise. However, for oscillators, the effect of vibration on the AM noise is reduced due to signal saturation inside the loop.

ACKNOWLEDGMENTS

The authors thank Dr. Fred Walls for useful discussions and comments. The authors also thank Jeff Jargon and Jennifer Taylor for their suggestions regarding the preparation of this manuscript.

REFERENCES

- [1] R. L. Filler, "The acceleration sensitivity of quartz crystal oscillators: A review," *IEEE Trans. Ultrason. Ferroelectr. Freq. Control*, vol. 35, no. 3, pp. 297–305, May 1988.
- [2] J. R. Vig, C. Audoin, L. S. Cutler, M. M. Driscoll, E. P. EerNisse, R. L. Filler, R. M. Garvey, W. L. Riley, R. C. Smythe, and R. D. Weglein, "Acceleration, vibration and shock effects—IEEE standards project P1193," in *Proc. 46th Annu. Frequency Control Symp.*, 1992, pp. 763–781.
- [3] R. L. Filler, J. A. Kosinski, and J. R. Vig, "Further studies on the acceleration sensitivity of quartz resonators," in *Proc. 37th Annu. Frequency Control Symp.*, 1983, pp. 265–271.
- [4] J. A. Kosinski and A. Ballato, "Designing for low acceleration sensitivity," *IEEE Trans. Ultrason. Ferroelectr. Freq. Control*, vol. 40, no. 5, pp. 532–537, Sep. 1993.
- [5] C. M. Jha, J. Salvia, S. A. Chandokar, R. Melamud, E. Kuhl, and K. W. Kenny, "Acceleration insensitive encapsulated silicon microresonator," *Appl. Phys. Lett.*, vol. 93, art. no. 324103, 2008.
- [6] J. Yang, X. Yang, J. A. Turner, J. A. Kosinski, R. A. Pastore, and W. Zhang, "Effects of middle plane curvature on vibrations of a thickness-shear mode crystal resonator," *Int. J. Solids Struct.*, vol. 43, pp. 7840–7851, 2006.
- [7] R. T. Wang and G. J. Dick, "High stability 40 Kelvin cryo-cooled sapphire oscillator," in *Proc. Joint Meeting of EFTF and IEEE FCS*, 2003, pp. 371–375.
- [8] L. D. Clayton and E. P. EerNisse, "Four-point SC-cut crystal unit design calculations for reduced acceleration sensitivity," in *Proc. IEEE Frequency Control Symp.*, 1992, pp. 582–596.
- [9] T. Nazarova, F. Riehle, and U. Sterr, "Vibration-insensitive reference cavity for an ultra-narrow-linewidth laser," *Appl. Phys. B*, vol. 83, no. 4, pp. 531–536, 2006.
- [10] V. J. Rosati and R. L. Filler, "Reduction of the effects of vibration on SC-Cut quartz crystal oscillators," in *Proc. IEEE Frequency Control Symp.*, 1981, pp. 117–121.
- [11] M. Bloch, O. Mancini, and C. Stone, "Method for achieving highly reproducible acceleration insensitive quartz crystal oscillators," U.S. Patent 07106143, Sep. 12, 2006.
- [12] D. A. Howe, J. Lanfranchi, L. Cutsinger, A. Hati, and C. W. Nelson, "Vibration-induced PM noise in oscillators and measurements of correlation with vibration sensors," in *Proc. IEEE Frequency Control Symp.*, 2005, pp. 494–498.
- [13] M. M. Driscoll, "Reduction of quartz oscillator flicker-of-frequency and white phase noise (floor) levels of acceleration sensitivity via use of multiple resonators," *IEEE Trans. Ultrason. Ferroelectr. Freq. Control*, vol. 40, no. 4, pp. 427–430, Jul. 1993.
- [14] H. Freuhauf, "g-Compensated, miniature, high performance quartz crystal oscillators," in *Proc. 38th Annu. PTTI Meeting*, 2007, pp. 251–258.
- [15] J. A. Kosinski, "Theory and design of crystal oscillators immune to acceleration: Present state of the art," in *Proc. IEEE/EIA Frequency Control Symp. and Exhibit.*, 2000, pp. 260–268.
- [16] D. S. Steinberg, *Vibration Analysis for Electronic Equipment*. New York: Wiley, .
- [17] M. M. Driscoll and J. B. Donovan, "Vibration-induced phase noise: It isn't just about the oscillator," in *Proc. Joint Meeting of European Frequency and Time Forum and IEEE Frequency Control Symp.*, 2007, pp. 535–540.
- [18] D. B. Leeson, "A simple model of feed back oscillator noise spectrum," in *Proc. IEEE*, vol. 54, no. 2, pp. 329–330, 1966.
- [19] A. Hati, C. W. Nelson, D. A. Howe, N. Ashby, J. Taylor, K. M. Hudek, C. Hay, D. Seidel, and D. Eliyahu, "Vibration sensitivity of microwave components," in *Proc. Joint Meeting of European Frequency and Time Forum and IEEE Frequency Control Symp.*, 2007, pp. 541–546.
- [20] P. Stockwell, C. McNeilage, M. Mossammaparast, D. M. Green, and J. H. Searls, "3-axis vibration performance of a compact sapphire microwave oscillator," in *Proc. IEEE Frequency Control Symp and PDA Exhibit.*, 2001, pp. 695–698.
- [21] J. C. Nallatamby, M. Prigent, M. Camiade, and J. J. Obregon, "Extension of the Leeson formula to phase noise calculation in transistor oscillators with complex tanks," *IEEE Trans. Microw. Theory Tech.*, vol. 51, no. 3, pp. 690–696, Mar. 2003.
- [22] F. L. Walls and E. S. Ferre-Pikal, "Measurement of frequency, phase noise and amplitude noise," in *Wiley Encyclopedia of Electrical and Electronics Engineering*. 1999, vol. 12, pp. 459–473.
- [23] E. Rubiola, M. Bruno, G. Lorino, and A. De Marchi, "Piezoelectric effect in coaxial cables," in *Proc. 11th European Frequency and Time Forum*, 1997, pp. 632–635.
- [24] J. Grove, J. Hein, J. Retta, P. Schweiger, W. Solbrig, and S. R. Stein, "Direct-digital phase-noise measurement," in *Proc. IEEE Frequency Control Symp.*, 2004, pp. 287–291.
- [25] C. E. Hay, M. E. Harrell, and R. J. Kansy, "2.4 and 2.5 GHz miniature, low-noise oscillators using surface transverse wave resonators

and a SiGe sustaining amplifier,” in *Proc. IEEE Frequency Control Symp.*, 2004, pp. 174–179.

- [26] A. Hati, D. A. Howe, and C. W. Nelson, “Comparison of AM noise in commercial amplifiers and oscillators at X-band,” in *Proc. IEEE Frequency Control Symp.*, 2006, pp. 740–744.
- [27] T. E. Parker and G. K. Montress, “Precision surface-acoustic-wave (SAW) oscillators,” *IEEE Trans. Ultrason. Ferroelectr. Freq. Control*, vol. 35, no. 3, pp. 342–364, May 1988.



Archita Hati was born in West Bengal, India, on April 26, 1970. She received her B.Sc., M.Sc., and Ph.D. degrees in physics from the University of Burdwan, West Bengal, India, in 1990, 1992, and 2001, respectively. She also received her M. Phil. in microwaves from the same university in 1993. Her Ph.D. work involved studies on high-performance frequency synthesizers and related problems.

Since May 2001, she has been a guest researcher with the Time and Frequency Metrology Group of the National Institute of Standards and Technology and the Physics Laboratory’s Time and Frequency Division. Her field of research includes phase noise metrology, low-noise frequency synthesis, low-noise microwave, and opto-electronic oscillators and vibration analysis. She also provides calibration services for the Time and Frequency Metrology Group. She has published more than 50 scientific papers.



Craig W. Nelson is an electrical engineer at the Time and Frequency Division of the National Institute of Standards and Technology. He received his BSEE degree from the University of Colorado in Boulder in 1990. After co-founding SpectraDynamics, a supplier of low-phase noise components, he joined the staff at the National Institute of Standards and Technology (NIST). He has worked on synthesis and control electronics, as well as software for both the NIST-7 and F1 primary frequency standards. He is presently involved in re-

search and development of ultra-stable synthesizers, low-phase noise electronics, and phase noise metrology. Current areas of research include optical oscillators, pulsed-phase noise measurements, and phase noise metrology in the 100-GHz range. He has published more than 40 papers and teaches classes, tutorials, and workshops at NIST, the IEEE Frequency Control Symposium, and several sponsoring agencies on the practical aspects of high-resolution phase noise metrology.



David A. Howe is leader of the Time and Frequency Metrology Group of the National Institute of Standards and Technology (NIST) and the Physics Laboratory’s Time and Frequency Division. His expertise includes spectral estimation using digital processing techniques, spectral purity and noise analysis, digital servo design, automated accuracy evaluation of primary cesium standards, atomic beam analysis, reduction of oscillator acceleration sensitivity for special applications, statistical theory, and clock-ensemble algorithms.

Mr. Howe has B.A. degrees in physics and math from the University of Colorado, Boulder, CO. He is a member of Sigma Pi Sigma and Phi Beta Kappa academic societies and an IEEE Senior Member. In 1970, he joined NIST (then NBS) Time Dissemination Research Section. From 1973 to 1984, he worked in the Atomic Standards Section doing advanced research on cesium and hydrogen maser standards and ruggedized, compact rubidium and ammonia standards. He returned to the Dissemination Research Section in 1984 to lead and implement several global high-accuracy satellite-based time-synchronization experiments with other national laboratories. For this contribution, he was awarded the Commerce Department’s highest commendation, the Gold Medal, in 1990 for advancements in coordinated universal time (UTC.) From 1994 to 1999, he worked as a statistical analyst for the Time Scale Section, which maintains UTC(NIST) from an ensemble of laboratory atomic frequency standards. Mr. Howe is the developer of the Total and TheoH variances used in high-accuracy estimation of long-term frequency stability. He has written articles for more than 100 publications and holds two patents in subjects related to precise frequency standards, timing, and synchronization.